Impact of Glycerol as Scavenger for Solar Hydrogen Production from Water

Chong Fai Kait, Ela Nurlaela, and Binay K. Dutta

***Abstract*—** The photocatalytic activity of titania supported bimetallic Cu-Ni photocatalysts was assessed and optimized for hydrogen production from water under visible light illumination (12.2 klux intensity). Research parameters investigated include total metal loading and Cu:Ni mass composition of the photocatalysts. The best performing photocatalyst was 10 wt% Cu-Ni/TiO_2 with Cu:Ni mass composition of 9:1, producing 6.1 mL of hydrogen over 2 hr reaction time. The impact of glycerol addition as hole-scavenger on the efficiency of solar hydrogen production from water was also investigated. Addition of 2.0 mL of glycerol to 8.0 mL of water enhanced the solar hydrogen production from 6.1 mL to 9.5 mL. If metal was not incorporated onto TiO_2, the hydrogen production was minimal, 2.0 mL after 2 hr reaction. The absorption spectra of metal-incorporated photocatalysts were not only enhanced in the UV region, they were also shifted to the visible region. All band gaps of the metal-incorporated photocatalysts were reduced compared to P25 TiO_2 (3.16 eV). The lowest band gap of 2.78 eV was displayed by 10 wt% Cu-Ni/TiO_2 bimetallic photocatalyst. Photooxidation of glycerol produced glyceraldehyde, glycolic acid and oxalic acid as intermediates.

***Keywords*—**Cu-Ni bimetallic, solar hydrogen, visible light, glycerol

I. Introduction

HYDROGEN can be produced from various processes and the production trend is moving from fossil fuels feedstock into renewable resources [1]. Solar hydrogen production from water offers an attractive and sustainable option since water is in abundance and the energy source from the sun is free. Titania, TiO_2 is the most popular photocatalyst used for solar hydrogen production due to its excellent chemical and phtochemical stability [2]. However, due to its high band gap, the efficiency in visible light is low. The low efficiency of photohydrogen production is mainly due to the inability of TiO_2 to utilize visible light. The bandgap of TiO_2 is about 3.2 eV meaning that it can only be activated by photons with wavelength less than 400 nm (UV region). Since solar radiation consists of 3-4% UV component, visible light-active photocatalyst is a crucial requirement for economically feasible hydrogen production.

The low efficiency of photohydrogen production was also due to the recombination reaction of photogenerated electrons and holes. Research on reducing the band gap has been vigorously conducted on water system by the incorporation of nonmetal [3] and metal components [4], [5] and also with the addition of hole-scavengers [6], [7]. Some metals such as Cu, Ag, Au Ni, Rh, Pt and Zn were capable to increase the catalytic activity of the photocatalyst, therefore enhancing the hydrogen production efficiency [8], [9]. Supported bimetallic catalysts have been widely used in industrial fields [10]. Bimetallic Cu-Ni has been reported to enhance carbon dioxide hydrogenation [11] and also photocatalytic reduction of nitrates [12].

Hole-scavengers are chemical species added into a photocatalytic system in order to stabilize the photogenerated holes. This is carried out in order to prevent the electron-hole recombination process. They are usually easily oxidized organic compounds. The literature has reported using formaldehyde, acetaldehyde, formic acid, acetic acid, methanol, ethanol, 2-propanol, butanol and azo dye as hole scavengers [13]–[15]. Since the hole scavengers will undergo oxidation process, it would be beneficial if value-added products could be produced from the photoreaction.

Glycerol is a by-product from transesterification of fats and oils to produce biodiesel. It is also produced from the hydrolysis process of palm oil (or other fats and oils) in soap and fatty acids manufacturing. The increasing demand for biodiesel has caused an oversupply of glycerol. Therefore, it would be advantageous to add-value to the glycerol by-product. The photo-oxidation of glycerol has been conducted using titania, TiO_2 [16], [17] under the irradiation of UV light to produce useful chemicals such as dihydroxyacetone, glycolaldehyde, glyceraldehyde, formic acid and CO_2. Besides the production of glycerol derivatives, hydrogen has also been produced using TiO_2 doped with Pt [18], Au and Pd [19], Cu [20]–[22] and Ni [22]. However, the reactions were conducted under the irradiation of UV light. The reaction scheme of glycerol oxidation is shown in Scheme 1 [23]. The

This work was supported in part by the Ministry of Science, Technology and Innovation, Malaysia, under the E-Science Fund Scheme (03-02-02-SF0002) and also by Universiti Teknologi PETRONAS.

Chong Fai Kait is with the Department of Fundamental and Applied Sciences, Universiti Teknologi PETRONAS, Bandar Seri Iskandar, 31750 Tronoh, Perak, Malaysia (phone: +6053687688; fax: +6053655905; email: chongfaikait@petronas.com.my).

Ela Nurlaela is from Indonesia and has completed her MSc (Chemical Engineering) in 2011 from Universiti Teknologi PETRONAS, Bandar Seri Iskandar, 31750 Tronoh, Perak, Malaysia (email: ela.jambari@gmail.com).

Binay K. Dutta is the Chariman of the West Bengal Pollution Control Board, Paribesh Bhawan, Salt Lake, Kolkata 700 098, India (email: chairman@wbpcb.gov.in).

intermediates generated during the oxidation process, to name a few, may include glyceraldehyde, dihydroxyacetone, glyceric acid, glycolic acid, mesooxalic acid and oxalic acids.

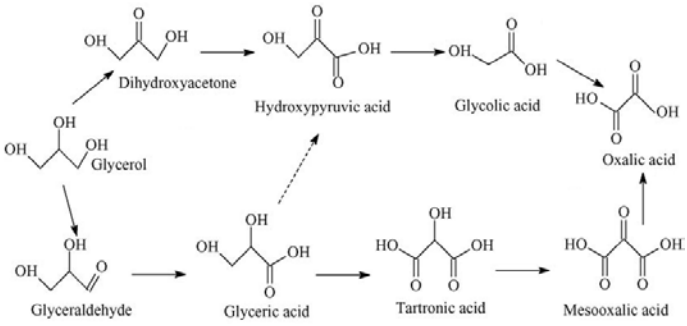

Scheme 1. Reaction scheme of glycerol oxidation [23]

In this study, bimetallic 10 wt%Cu-Ni/TiO_2 and monometallic 10 wt%Cu/TiO_2 and 10 wt%Ni/TiO_2 photocatalysts were prepared, characterized and investigated for solar hydrogen production under visible light. The effect of total bimetal loading and Cu:Ni mass composition on the efficiency of solar hydrogen production was also investigated. It is expected that by metal doping, the activity region of the photocatalyst will be shifted to the visible light region. The addition of glycerol, which acts as a hole-scavenger will be able to enhance the hydrogen production efficiency. Products from the photooxidation process were also analyzed.

II. Materials and Methods

A. Preparation of Cu-Ni/TiO_2 Photocatalyst

Degussa P25 TiO_2 was used as the support for all the photocatalysts prepared. Bimetallic photocatalysts with 10 wt% total metal loading were prepared via co-precipitation method to investigate the effect of Cu:Ni mass composition (9:1, 7:3 and 5:5) on solar hydrogen production efficiency. The monometallics 10 wt% Cu/TiO_2 (Cu:Ni, 10:0 mass composition) and 10 wt% Ni/TiO_2 (Cu:Ni, 0:10 mass composition) were also prepared in addition to P25 TiO_2 used as references. The metal precursors were copper(II) nitrate trihydrate, $Cu(NO_3)_2.3H_2O$ (Acros, >98% purity) and nickel(II) nitrate hexahydrate, $Ni(NO_3)_2.6H_2O$ (Acros, >98% purity). Glycerol (Systerm, 95% purity) was used as a templating agent while sodium hydroxide, NaOH (Merck, 95%), was added as the precipitating agent. All the materials were used as received without further purification. Known amounts of $Cu(NO_3)_2.3H_2O$ and/or $Ni(NO_3)_2.6H_2O$ were weighed and dissolved in distilled water followed by the addition of glycerol. The solution was stirred continuously prior to addition of TiO_2. The slurry was stirred for another hour before adding 0.25 M NaOH dropwise until pH = 12 to form precipitates. The mixture was aged for 1 day, filtered and dried overnight at 75°C in an oven. Calcination was conducted at 200°C for 1 hr. The effect of total metal loading (5 wt%, 9 wt%, 10 wt%, 11 wt% and 15 wt%) for photocatalysts with Cu:Ni, 9:1 mass composition on the performance for solar hydrogen production was also investigated. The drying and calcination temperatures and durations were selected based on previous study reported elsewhere [24].

B. Characterization of Cu-Ni/TiO_2 Photocatalyst

The bimetallic, monometallic and TiO_2 photocatalysts were characterized using powder X-ray diffraction (XRD), field emission scanning electron microscopy (FESEM) temperature-programmed reduction (TPR) and diffuse reflectance UV-Vis spectroscopy (DRUV-Vis).

The photocatalysts were analysed for the type of TiO_2 phases present using Bruker D8 Advance with CuKα radiation (40 kV, 40 mA) at 2θ angles from 10° to 80°, with a scan speed of 4°·min^{-1}. Crystallite size of TiO_2 phase can also be calculated from the XRD data. The morphology of the photocatalysts such as particle shape, size, and size distribution were analyzed using FESEM. The analyses were conducted using Zeiss Supra 35VP with 80 kX magnification and operating at 10 kV.

Temperature-programmed reduction (TPR) was carried out on the photocatalysts to determine the type of reducible species present. The analyses were conducted using the Thermo Finnigan TPDRO 1100 equipment. Calcined photocatalyst samples were first pretreated for 30 min at 110°C with a ramp rate of 10°C·min^{-1} under nitrogen flow of 20 mL·min^{-1}. After cooling down to room temperature, TPR was carried out from 40-800°C ramping at 10°C·min^{-1} in 5% H_2/N_2 with a flow rate of 20 mL·min^{-1}. The TPR results were displayed as reduction profiles with the amount of H_2 consumed versus temperature. DRUV-Vis measurement was performed using a Shimadzu Spectrometer 3150, equipped with an integrating sphere. $BaSO_4$ was employed as the reference material with analysis ranging from 190 to 800 nm. This technique is used to determine any shifting of the absorption edge to the visible region for the photocatalysts due to metal incorporation. The band gap energies of the photocatalysts could be determined from the Kubelka-Munk function, F(R), using the Tauc plot, a plot of $(F(R).hv)^{1/2}$ against hv.

C. Solar Hydrogen Production

The photocatalysts were evaluated for solar hydrogen production using a multiport photoreactor integrated to water displacement units (Fig. 1) to measure the volume of gaseous product(s). A 500 W halogen lamp was used to simulate visible light, irradiating the photoreactor from the top giving an intensity of 12.2 klux. The top cover of the photoreactor is made from a flat piece of quartz material. Due to the heat released from the lamp, a cooling fan was stationed next to the photoreactor in order to maintain the temperature of the photoreaction.

A 0.1 g of photocatalyst powder was suspended in distilled water (8.0 mL) and placed in the multiport photoreactor. The

amount of gas evolved was monitored for 2 hr. The gaseous product was analyzed using a gas chromatograph (Agilent 6890 series GC system) with 5A molecular sieve column (capillary 45.0 m × 530 µm × 25 µm) and equipped with thermal conductivity detector. Helium gas was used as the carrier gas.

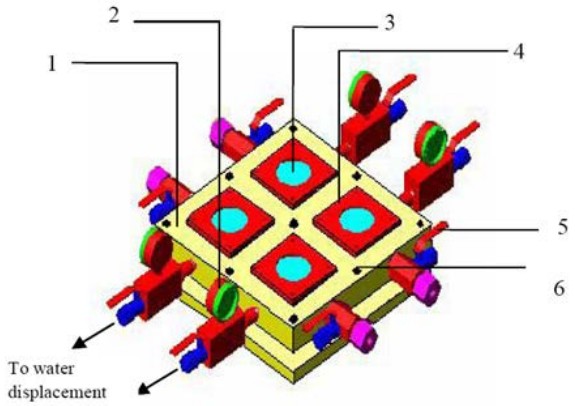

Key: 1. Acrylic board; 2. Pressure gauge; 3. Quartz disk; 4. Square metal plate; 5. One way valve; 6. Screw

Fig. 1. Schematic of the multiport photoreactor

For experiments where liquid glycerol was added to study its effect as hole-scavenger in solar hydrogen production from water, the volume of glycerol was varied from 2.0 mL to 8.0 mL. Products from the photooxidation process were analyzed using high performance liquid chromatography (HPLC) (Agilent 1100 series) equipped with a Transgenomic column (ICE-ORH-801) and using 0.01 N H_2SO_4 as eluent. The flow rate of the eluent was set at 0.8 mL·min^{-1}. Standard solutions of possible intermediate products were calibrated for both qualitative and quantitative determination. These intermediates were glycolic acid, formic acid, oxalic acid, mesooxalic acid and glyceraldehyde. Finally, the outlet of the photoreactor was connected to a calcium hydroxide solution prior to the water displacement units to detect any presence of carbon dioxide during photoreaction.

III. Results and Discussion

A. Preparation of Cu-Ni/TiO_2 Photocatalyst

Bimetallic photocatalysts were prepared to investigate the effects of Cu:Ni mass composition, and total metal loading on the performance for solar hydrogen production from water. The 10 wt% monometallic photocatalysts were also prepared. Calcination was conducted at 200°C for 1 hr duration. These pretreatment conditions were the optimum conditions selected based on previous work [24]. The photocatalysts were given denotation of 10 wt%_9Cu1Ni for the bimetallic photocatalyst with 9:1 Cu:Ni mass composition while 5 wt%_9Cu1Ni and 15 wt%_9Cu1Ni were referred to bimetallic photocatalysts (Cu:Ni mass composition of 9:1) with 5 wt% and 15 wt% total metallic loading, respectively. On the other hand, 10 wt%_10Cu and 10 wt%_10Ni were used to refer to the monometallic Cu and Ni photocatalysts, respectively.

B. Characterization of Cu-Ni/TiO_2 Photocatalyst

Characterization procedures were conducted to determine the bulk and surface properties of the photocatalysts.

1) XRD

Fig. 2 shows the XRD patterns of the photocatalysts and TiO_2. The peaks were mainly characteristic peaks of the anatase phase at 2θ = 25.3°, 33.8°, 47.8°, 53.8° and 55.0°, while the rutile phase was represented by peaks at 2θ = 27.4° and 41.5°. It was found that no characteristic peaks representing Cu-, Ni- or CuNi-species could be detected indicating that the metal particles were well dispersed on TiO_2. This observation was also true for the bimetallic photocatalysts with 15 wt% metal loading. The presence of glycerol during photocatalyst preparation may have contributed to the high metal dispersion [25], [26]. The average crystallite size calculated using Scherrer equation was 35 nm.

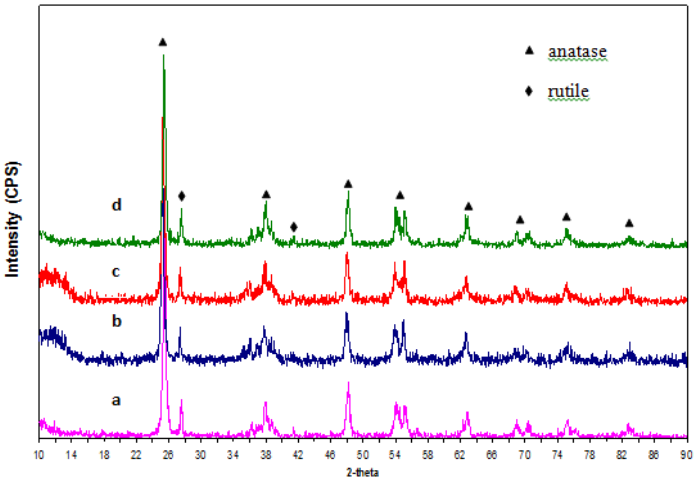

Fig. 2. XRD patterns of (a) TiO_2, (b) 10 wt%_9Cu1Ni, (c) 10 wt%_10Cu, and (d) 10 wt%_10Ni

2) FESEM

The FESEM images represented in Fig. 3 shows that the photocatalysts were present as uniform spherical shaped particles. All the photocatalysts tend to display slight agglomeration. This may be due to the presence of NaOH during photocatalyst preparation and pretreatment (calcination). The particle size of the photocatalysts ranged from 20-40 nm, the observation is in good agreement with the crystallite size calculated from the XRD data. However, no indication of localized metal deposition was observed, which was also confirmed by the XRD results. The observation may be due to the presence of highly dispersed metal particles with size range which are below the detection limit of both equipments [26].

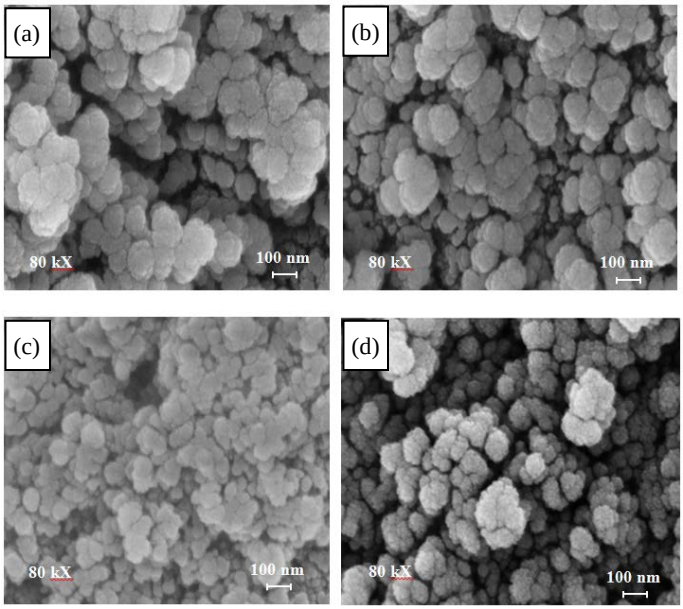

Fig. 3. FESEM images of (a) 10 wt%_9Cu1Ni, (b) 10 wt%_10Cu, (c) 10 wt%_10Ni, and (d) TiO_2

3) TPR

The TPR profiles of the monometallic and bimetallic 10 wt%_9Cu1Ni photocatalysts are presented in Fig. 4. Monometallic 10 wt%_10Cu displayed two distinct reduction peaks. The peak at 205°C is attributed to reduction of highly dispersed CuO particles with less interaction with TiO_2 support [27], while the higher temperature reduction peak at 256°C may be attributed to reduction of larger CuO particles having stronger interaction with TiO_2 [26], [27]. On the other hand, monometallic 10 wt%_10Ni showed a broad reduction peak at 381°C attributed to reduction of NiO having strong interaction with TiO_2 [28].

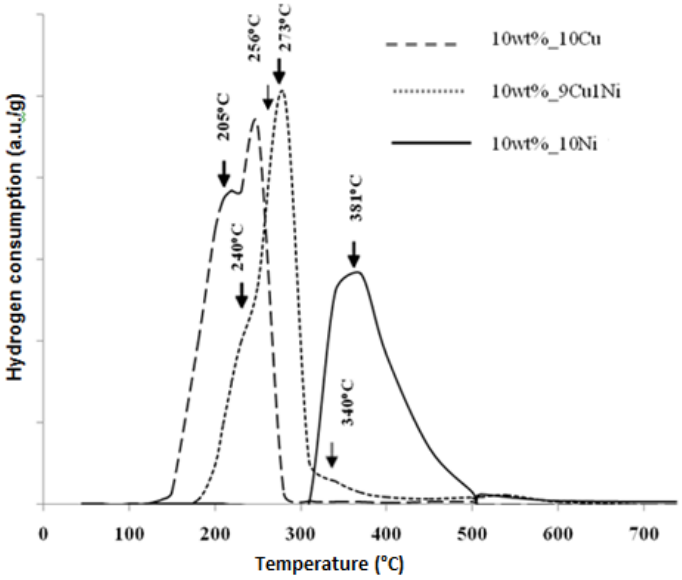

Fig. 4. TPR profiles of monometallic and bimetallic photocatalysts

However, the reduction profile of the bimetallic photocatalyst did not resemble any of the monometallic photocatalysts. This indicates that the bimetallic photocatalyst does not have segregated CuO and NiO particles similar to those in the monometallics. A dominant reduction peak was observed at 273°C and two shoulders at 240°C and 340°C. The presence of Ni has shifted the reduction of CuO to higher temperature, from 205°C to 240°C. At the same time, the reduction of NiO seemed to be catalyzed by the presence of Cu as indicated by the distinct peak at 273°C and the disappearance of the peak at 381°C. Such phenomenon is observed when Cu-Ni mixed oxide particles are co-reduced during the analysis [29], [30].

4) DRUV-Vis

DRUV-Vis spectrum of P25 TiO_2 in Fig. 5 showed its absorption edge at 400 nm. No absorption was observed in the visible region (*f* 400 nm). However, the edge shifted to the visible region with the addition of 10 wt% Cu, Ni or Cu-Ni indicating reduction in band gap values.

The presence of metal not only increased the visible light absorption, it also enhanced the absorbance in the UV region (wavelength < 400 nm) as indicated by the higher absorbance of the bimetallic and monometallic photocatalysts [32], [33] compared to TiO_2 in Fig. 5. In the UV region, the 10 wt%_10Ni monometallic photocatalyst displayed the highest absorbance of *approx.* 0.19 followed by both 10 wt%_10Cu and 10 wt%_9Cu1Ni, and finally by TiO_2 displaying the lowest absorbance (*approx.* 0.1). The presence of Ni in 10 wt%_9Cu1Ni seemed to enhance its visible light harvesting property. The bimetallic 10 wt%_9Cu1Ni photocatalyst displayed the highest absorbance in the visible light region, and extending through to 800 nm. This was followed by 10 wt%_10Cu and 10 wt%_10Ni photocatalysts, which displayed minimal absorbance. Finally, TiO_2 displayed zero absorbance in the visible region.

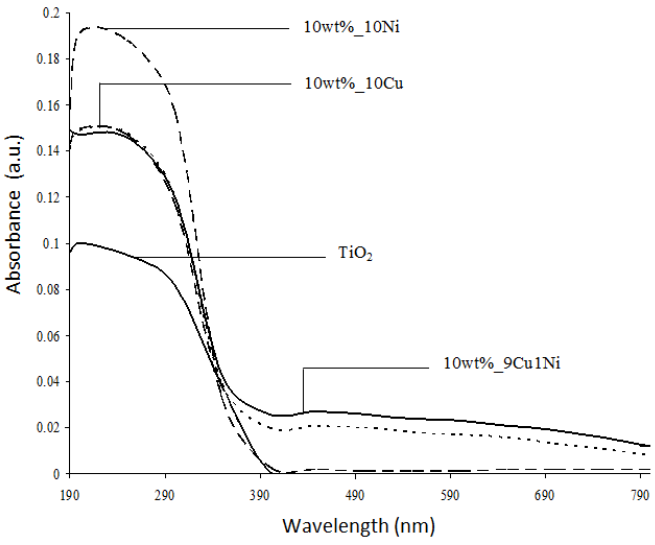

Fig. 5. DRUV-Vis spectra of the monometallic and bimetallic photocatalysts

Surface modification of TiO_2 with Cu, Ni or Cu-Ni could significantly reduce the band gap thus shifting the absorption edge to the visible region [31]–[34]. Using Tauc plot (not shown), the band gaps were calculated and displayed in TABLE I. TiO_2 has the highest band gap of 3.16 eV. The incoporation of monometallic Cu or Ni reduced the band gap to 2.98 eV for both photocatalysts. The lowest band gap was displayed by 10 wt%_9Cu1Ni, 2.78 eV.

Fig. 6 represents the DRUV-Vis spectra of the bimetallic photocatalysts (Cu:Ni, 9:1 mas composition) with different total metal loading in comparison with TiO_2. The presence of bimetal obviously increased the absorption in both the UV and visible light region. This result was in good agreement with the reported literatures. Komova *et al.* [32] observed that the absorption spectra of Cu/TiO_2 photocatalyst shifted to the visible region as the copper content increased. This might be due to the growth of oxide clusters caused by the aggregation of copper particles. As a result of this phenomenon, the axial Cu-O bonds weaken while the in-plane Cu-O bonds strengthen, leading to a blue shift due to the d-d transition. It was also reported by Begum *et al.* [33] that increasing the nickel content led to the absorption band shifted to the longer visible wavelength.

When 5 wt% bimetal was incorporated onto TiO_2, the absorption in the UV region was enhanced to *approx.* 0.23. However, the absorbance in the visible range was not significantly increased. On the other hand, when 10 wt% bimetal was added, the absorbance in the visible region was enhanced at the cost of the absorbance in the UV region. The photocatalyst with 15 wt% total metalic loading displayed the highest absorption in the visible region with slightly higher enhancement in the UV region when compared to the photocatalyst with 10 wt% metal loading.

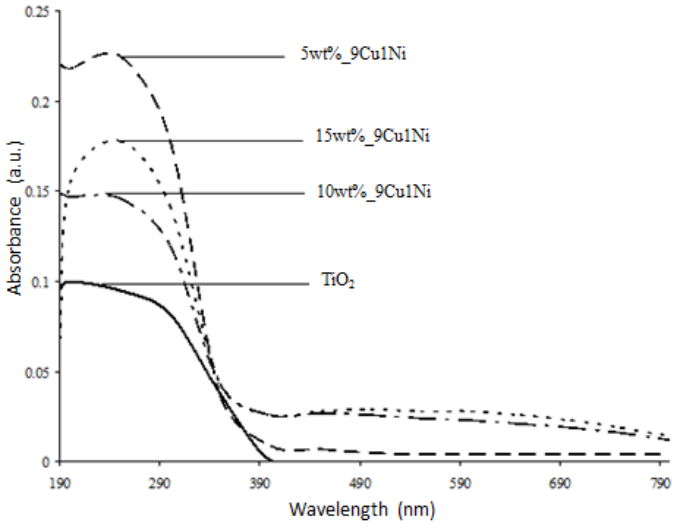

Fig. 6. DRUV-Vis spectra of the bimetallic photocatalysts with different total metal loading

However, in the case of calculated band gap energy in TABLE I, 10 wt% bimetallic photocatalyst showed the lowest band gap energy (2.78 eV), slightly lower the band gap for 15 wt% bimetallic photocatalyst (2.85 eV). Although the 5 wt% bimetallic photocatalyst displayed the highest absorption in the UV region, it showed the lowest absorption in the visible region with calculated band gap of 3.15 eV.

TABLE I. BAND GAP OF PHOTOCATALYSTS

Photocatalyst	Band gap, eV
TiO_2	3.16
10wt%_10Cu	2.98
5wt%_9Cu1Ni	3.15
10wt%_9Cu1Ni	2.78
15wt%_9Cu1Ni	2.85
10wt%_7Cu3Ni	2.98
10wt%_5Cu5Ni	3.05
10wt%_10Ni	2.98

C. Solar Hydrogen Production

Referring to Fig. 7, the effect of Cu:Ni mass composition on the solar hydrogen production efficiency was investigated. Bimetallic 10 wt%_9Cu1Ni photocatalyst displayed the highest hydrogen production of 6.1 mL compared to monometallic 10 wt%_10Cu and 10 wt%_10Ni photocatalysts, giving 5.0 mL and 4.3 mL, respectively. TiO_2 was able to produce only 2.0 mL hydrogen gas. The reduction in band gap values (Table I) for the metal-incorporated photocatalysts compared to TiO_2 has led to an increase in hydrogen production from water. This is caused by the enhancement in the visible light-harvesting property of the metal-incorporated photocatalysts.

The addition of small amount of Ni onto Cu/TiO_2 (10 wt%_9Cu1Ni) was able to enhance the performance of the photocatalyst from producing 5.0 mL to 6.1 mL hydrogen. This may be due to Cu acting as both hole- and electron-traps [35] while Ni as hole-trap only [36]. The synergy between Cu-Ni as hole- and electron-traps led to enhancement in stabilizing the spatial charge separation [12]. Based on the reduction profile displayed in Fig. 5, coreduction of the Cu-Ni mixed oxides was observed where the presence of Cu catalyzes the reduction of NiO to lower temperature [29]. However, as the composition of Ni increased, Cu:Ni mass composition varied from 7:3 to 5:5, detrimental effect was observed resulting in lower amount of hydrogen produced compared to 10 wt%_9Cu1Ni. The increase in the amount of Ni led to it becoming the hole-accumulation site which could attract the photogenerated electrons causing electron-hole recombination. The observation agrees with the band gap values tabulated in

TABLE I, as the composition of Ni increased, the photocatalytic activity in the visible light region decreased, therefore, the band gap values increased from 2.98 eV to 3.05 eV for 10 wt%_7Cu3Ni to 10 wt%_5Cu5Ni, respectively.

During photoreaction, hydrogen should be produced together with oxygen. However, no oxygen was detected from the gas chromatography. This may be attributed to the oxygen itself acting as an electron acceptor leading to the formation of superoxide radical anions [37]. This may retard the continuous production of hydrogen causing the deactivation of the photocatalyst.

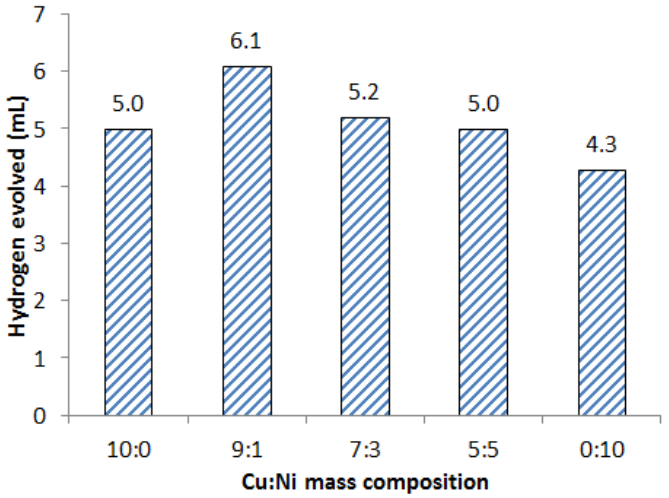

Fig. 7. The effect of Cu:Ni mass composition of photocatalyst with 10 wt% total metal loading on hydrogen production

Fig. 8 revealed that as the total metal loading of the bimetallic photocatalysts (Cu:Ni mass composition of 9:1) was increased from 5 wt% to 10 wt%, the amount of hydrogen gas evolved increased from 3.0 mL to 6.1 mL. The presence of metal was able to inhibit the electron-hole recombination process [38].

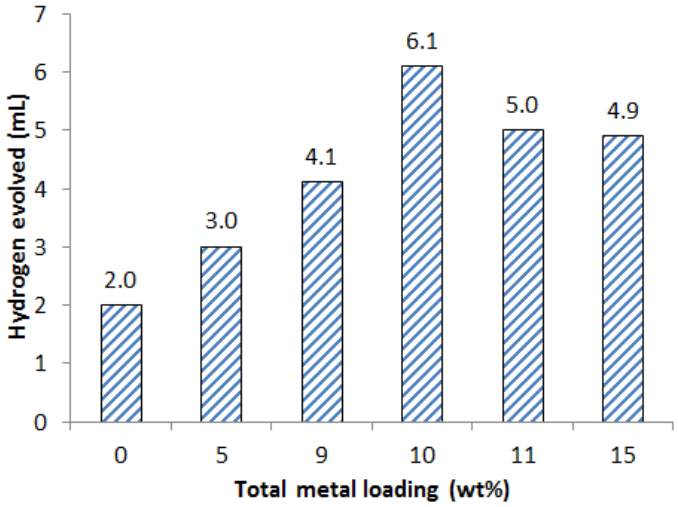

Fig. 8. The effect of total metal loading of photocatalyst (Cu:Ni mass composition 9:1) on hydrogen production

However, when the total metal loading was increased to 11 wt%, the photocatalytic activity was reduced to 5.0 mL hydrogen evolved. Further increase in total metal loading showed lowered performance. As the total metal loading increases, the metal sites will act as electron-hole recombination centers due to electrostatic forces between the negatively charged metal sites and the positively charged holes [38], [39]. The trend in the performance for the bimetallic photocatalyst increased from 5 wt%, 15 wt% and 10 wt%; in agreement with the decreasing value in the band gaps; 3.15 eV, 2.85 eV and 2.78 eV, respectively. The optimum loading for bimetallic Cu-Ni was 10 wt%.

From Fig. 9, the effect of glycerol amount on hydrogen production was investigated using 10 wt%_9Cu1Ni. When 2.0 mL of glycerol was added, tremendous increase in the amount of hydrogen produced (9.5 mL) was observed. At this stage glycerol acts as a hole scavenger [21] diminishing the effect of electron-hole recombination. Although the amount of hydrogen produced decreased when more glycerol was added, the overall effect was enhancement of performance compared to without glycerol addition. The decreased performance with higher amount of glycerol may be due to the competitive adsorption of glycerol, its intermediates and water onto the photocatalyst surface [40].

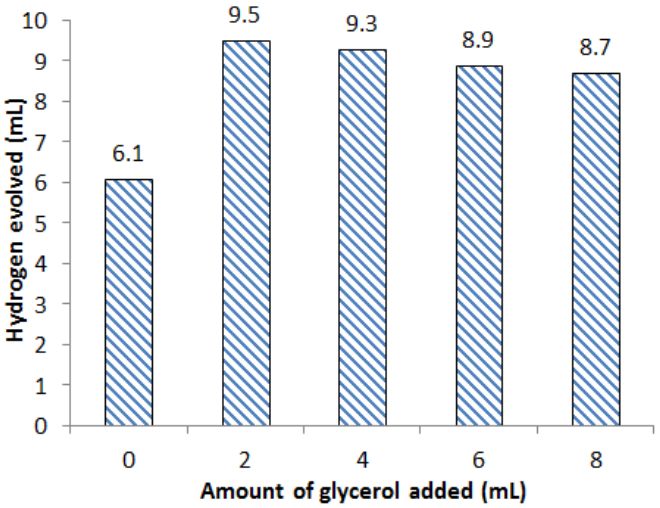

Fig. 9. The effect of glycerol amount on hydrogen production using 10 wt%_9Cu1Ni

The intermediate products identified from glycerol photooxidation were mainly glyceraldehyde and glycolic acid, only traces of oxalic acid was detected [18]. No carbon dioxide was detected during the reaction even when the reaction time was extended to 50 hr. It has been reported that complete mineralization of glycerol into carbon dioxide could only occur for prolonged photoreaction of more than 100 h [41]. The use of glycerol as sacrificial agent for hydrogen production from water serves not only to enhance the photocatalytic performance but it also contributed to the generation of value-added products from the biodiesel by-product.

IV. Conclusion

The photocatalysts displayed high metal dispersion based on the analysis from XRD and also FESEM. Particles were of spherical shape with slight agglomeration with size ranging from 20-40 nm. The addition of Cu, Ni or bimetallic Cu-Ni onto TiO_2 led to reduction in band gap. The best performing photocatalyst was 10 wt%_9Cu1Ni with its optimum Cu:Ni mass composition of 9:1 and optimum bimetallic loading of 10 wt%. The band gap was reduced from 3.16 eV (TiO_2) to 2.78 eV for 10 wt%_9Cu1Ni photocatalyst. This led to enhancement in the hydrogen production (6.1 mL) under visible light illumination compared to using TiO_2 (2.0 mL). The The addition of 2.0 mL of glycerol as hole-scavenger to 8.0 mL of water further enhanced the solar hydrogen production to 9.5 mL. The photooxidation of glycerol under visible light illumination produced glyceraldehyde, glycolic acid and oxalic acid.

Acknowledgment

The authors would like to acknowledge the Ministry of Science, Technology and Innovation (MOSTI), Malaysia, for the award of E-Science Fund Scheme (03-02-02-SF0002) and Universiti Teknologi PETRONAS for providing research facilities and financial support (graduate assistantship).

References

[1] M. Momirlan, and T. Veziroglu, "Recent directions of world hydrogen production", *Renewable and Sustainable Energy Reviews*, vol. 3, pp. 219-231, 1999.

[2] M. Ni, M.K.H. Leung, D.Y.C. Leung, and K. Sumathy, "A review and recent developments in photocatalytic water-splitting using TiO_2 for hydrogen production", *Renewable and Sustainable Energy Reviews*, vol. 11, pp 401-425, 2007.

[3] M. Kitano, M. Matsuoka, M. Ueshima, and M. Anpo, "Recent developments in titanium oxide-based photocatalysts", *Applied Catalysis A: General*, vol. 325, pp.1-14, 2007.

[4] A. Kudo, R. Niishiro, A. Iwase, H. Kato, "Effects of doping of metal cations on morphology, activity, and visible light response of photocatalysts", *Chemical Physics*, vol 339, pp.104-110, 2007.

[5] J.P. Yasomanee, and J. Bandara, "Multi-electron storage of photoenergy using Cu_2O–TiO_2 thin film photocatalyst", *Solar Energy Materials and Solar Cells*, vol. 92, pp.348-352, 2008.

[6] J. Premkumar, "Development of Super-Hydrophilicity on Nitrogen-Doped TiO_2 Thin Film Surface by Photoelectrochemical Method under Visible Light", Chemistry Materials, vol. 16, pp.3980-3981, 2004.

[7] J. Bandara, C.P.K. Udawatta, and C.S.K. Rajapakse, "Highly stable CuO incorporated TiO_2 catalyst for photocatalytic hydrogen production from H_2O", *Photochemical and Photobiological Sciences*, vol. 4, no. 11, pp. 857-861, 2005.

[8] G.L. Chiarello, E. Selli, L. Forni, "Photocatalytic Hydrogen Production Over Flame Spray Pyrolysis-synthesised TiO_2 and Au/TiO_2", *Applied Catalysis B: Environmental*, vol. 84, pp. 332–342, 2008.

[9] Z.M. El-Bahy, A.A. Ismail, R.M. Mohamed, "Enhancement of Titania by Doping Rare Earth for Photodegradation of Organic Dye (Direct Blue)", *Journal of Hazardous Materials*, vol. 166, no.1, pp. 138-143, 2008.

[10] V. Ponec, "Alloy catalysts: the concepts", *Applied Catalysis A: General*, vol. 222, pp. 31–45, 2001.

[11] Y. Liu, D. Liu, "Study of Bimetallic $Cu\text{-}Ni/Al_2O_3$ Catalysts for Carbondioxide Hydrogenation", *International Journal of Hydrogen Energy*, vol. 24, pp. 351-354, 1999.

[12] W. Gao, R. Jin, J. Chen, X. Guang, H. Zheng, F. Zhang, N. Guan, "Titania-supported Bimetallic Catalysts for Photocatalytic Reduction of Nitrate", *Catalysis Today*, vol. 90, pp. 331-336, 2004.

[13] B. Zielinska, E. Borowiak-Palen, and R.J. Kalenczuk, "Photocatalytic hydrogen generation over alkaline-earth titanates in the presence of electron donors," *International Journal of Hydrogen Energy*, vol. 33, pp. 1797 – 1802, 2008.

[14] A. Patsoura, D.I. Kondarides, and X.E. Verykios, "Enhancement of photoinduced hydrogen production from irradiated Pt/TiO_2 suspensions with simultaneous degradation of azo-dyes," *Applied Catalysis B*, vol. 64, pp. 171–179, 2006.

[15] A. Patsoura, D. I. Kondarides, and X.E. Verykios, "Photocatalytic degradation of organic pollutants with simultaneous production of hydrogen," *Catalysis Today*, vol. 124, pp. 94–102, 2007.

[16] V. Maurino, A. Bedini, M. Minella, F. Rubertelli, E. Pelizzetti, and C. Minero, "Glycerol Transformation Through Photocatalysis: A Possible Route to Value Added Chemicals", *Journal of Advanced Oxidation Technologies*, vol. 11, no. 2, pp. 184-192, 2008.

[17] V. Augugliaro, H.A. Hamed El Nazer, V. Loddo, A. Mele, G. Palmisano, L. Palmisano, and S. Yurdakal, "Partial photocatalytic oxidation of glycerol in TiO_2 water suspensions", Catalysis Today, vol. 151, no. 1-2, pp. 21-28, 2010.

[18] M. Li, Y. Li, S. Peng, G. Lu, and S.B. Li, 2009, "Photocatalytic hydrogen generation using glycerol wastewater over Pt/TiO_2", *Frontiers of Chemistry in China*, vol. 4, no.1, pp. :32-38, 2009.

[19] M. Bowker, P.R. Davies, and L.S. Al-Mazroai, "Photocatalytic Reforming of Glycerol over Gold and Palladium as an Alternative Fuel Source", *Catal Lett*, vol. 128, pp. 253-255, 2009.

[20] G. Li, N.M. Dimitrijevic, L. Chen, T. Rajh, and K.A. Gray, "Role of Surface/Interfacial Cu^{2+} Sites in the Photocatalytic Activity of Coupled CuO−TiO_2 Nanocomposites", *J. Phys. Chem, C*, vol. 112, pp. 19040-19044, 2008.

[21] V. Gombac, L. Sordelli, T. Montini, J.J. Delgado, A. Adamski, G. Adami, M. Cargnello, S. Bernal, and P. Fornasiero, "CuO_x−TiO_2 Photocatalysts for H_2 Production from Ethanol and Glycerol Solutions", *J. Phys. Chem, A*, vol. 114, pp. 3916-3925, 2010.

[22] A.V. Korzhak, N.I. Ermokhina, A.L. Stroyuk, V.K. Bukhtiyarov, A.E. Raevskaya, V.I. Litvin, S.Y. Kuchmiy, V.G. Ilyin, and P.A. Manorik, "Photocatalytic hydrogen evolution over mesoporous TiO_2/metal nanocomposites", *Journal of Photochemistry and Photobiology A: Chemistry*, vol.198, no. 2-3, pp. 126-134, 2008.

[23] C.L. Bianchi, P. Canton, N. Dimitratos, F. Porta, and L. Prati, "Selective oxidation of glycerol with oxygen using mono and bimetallic catalysts based on Au, Pd and Pt metals," *Catalysis Today*, vol. 102–103, pp. 203–212, 2005.

[24] E. Nurlaela, "Development of $Cu\text{-}Ni/TiO_2$ bimetallic catalyst for photohydrogen production under visible light illumination", M.Sc. Thesis, Universiti Teknologi PETRONAS, 2011.

[25] Y. Li, M. Cai, J. Rogers, Y. Xu, and W. Shen, "Glycerol-mediated synthesis of Ni and Ni/NiO core-shell nanoparticles," *Materials Letters*, vol. 60, pp. 750-753, 2006.

[26] L.S. Yoong, F.K. Chong, and B.K. Dutta, "Development of copper-doped TiO_2 photocatalyst for hydrogen production under visible light " *Energy*, vol. 34, pp. 1652-1661, 2009.

[27] W.P. Dow, Y.-P. Wang, and T.-J. Huang, "TPR and XRD studies of yttria-doped ceria/y-alumina-supported copper oxide catalyst," *Applied Catalysis A*, vol. 190, pp. 25–34, 2000.

[28] M. D. Romero, J. A. Calles, and A. Rodrguez, "Influence of the preparation method and metal precursor compound on the bifunctional Ni/HZSM-5 Catalysts," *Industrial and Engineering Chemistry Research*, vol. 37, pp. 3846–3852, 1998.

[29] P. Li, J. Liu, N. Nag, P.A. Crozier, "In Situ Preparation of $Ni\text{-}Cu/TiO_2$ Bimetallic Catalysts", *Journal of Catalysis*, vol. 262, pp. 73-82, 2009.

[30] R. Pe´rez-Hernandez, G. M. n. Galicia, D. M. Anaya, J. Palacios, C. Angeles-Chavez, and J. Arenas-Alatorre, "Synthesis and characterization of bimetallic $Cu–Ni/ZrO_2$ nanocatalysts: H_2 production by oxidative steam reforming of methanol," *International Journal of Hydrogen Energy*, vol. 33, pp. 4569 – 4576, 2008.

[31] J. Escobar, J. A. D. L. Reyes, and T. Viveros, "Nickel on TiO_2-modified

Al_2O_3 sol–gel oxides: Effect of synthesis parameters on the supported phase properties," *Applied Catalysis A*, vol. 253, pp. 151-163, 2004.

[32] O. V. Komova, A. V. Simakov, V. A. Rogov, D. I. Kochubei, G. V. Odegova, V. V. Kriventsov, E. A. Paukshtis, V. A. Ushakov, N. N. Sazonova, and T. A. Nikoro, "Investigation of the state of copper in supported copper–titanium oxide catalysts," *Journal of Molecular Catalysis A*, vol. 161, pp. 191-204, 2000.

[33] N. S. Begum, H. M. F. Ahmeed, and K. R. Gunashekar, "Effects of Ni doping on photocatalytic activity of TiO_2 thin films prepared by liquid phase deposition technique," *Bulletin of Material Science*, vol. 31, pp. 747–751, 2008.

[34] T. Umebayashi, T. Yamaki, H. Itoh, K. Asai, "Analysis of electronic structures of 3d transition metal-dope TiO_2 based on band calculation", *Journal of Physics and Chemistry Solids*, vol. 63, pp. 1909-1920, 2002.

[35] T. Miwa, S. Kaneco, H. Katsumata, T. Suzuki, K. Ohta, S.C. Verma, and K. Sugihara, "Photocatalytic hydrogen production from aqueous methanol solution with $CuO/Al_2O_3/TiO_2$ nanocomposite," *International Journal of Hydrogen Energy*, vol. 35, pp. 6554-6560, 2010.

[36] D. Jing, L. Guo, L. Zhao, "Study on the synthesis of Ni doped mesoporous TiO_2 and its photocatalytic activity for hydrogen evolution in aqueous methanol solution," *Chemical Physics Letters*, vol.415, pp. 74-78, 2005.

[37] D.H. Tseng, L.C. Juang and H.H. Huang, "Effect of oxygen and hydrogen peroxide on the photocatalytic degradation of monochlorobenzene in TiO_2 aqueous suspension", *International Journal of Photoenergy*, vol. 2012, pp. 1-9, 2012.

[38] O. Carp, C. L. Huisman, and A. Reller, "Photoinduced Reactivity of Titanium Dioxide", *Progress in Solid State Chemistry*, vol. 32, pp. 33-117, 2004.

[39] T. Sreethawong, S. Laehsalee, and S. Chavadej, "Use of Pt/N-doped mesoporous-assembled nanocrystalline TiO_2 for photocatalytic H_2 production under visible light irradiation", *Catalysis Communications*, vol. 10, pp. 538–543, 2009.

[40] S. Chavadej, P. Phuaphromyod, E. Gulari, P. Rangsunvigit, and T. Sreethawong, "Photocatalytic degradation of 2-propanol by using Pt/TiO_2 prepared by microemulsion technique", *Chemical Engineering Journal*, vol. 137, pp. 489–495, 2008.

[41] V.M. Daskalaki and D.I. Kondarides," Efficient production of hydrogen by photo-induced reforming of glycerol at ambient conditions"**,** *Catalysis Today*, vol. 144, pp. 75-80, 2009.